Model peptide studies of Ag+ binding sites from the silver resistance protein SilE†

V. Chabert, [ID] [a] M. Hologne, [ID] [b] O. Sénèque,[c] A. Crochet, [ID] [d] O. Walker [ID] [b] and K. M. Fromm [ID] *[a]

Using model peptides, each of the nine MX_2H or HX_nM (n = 1, 2) motifs of the silver resistance protein SilE has been shown to coordinate to one Ag+ ion by its histidine and methionine residues with K_d in the µM range. This suggests an Ag+ buffering role for SilE in the case of high Ag+ overload.

The silver cation Ag+ and its compounds have been known for their antibacterial properties.[1–3] However, an increasing number of reports have highlighted the emergence of silver resistant bacterial strains isolated from burn care centers or silver contaminated media.[4–6] This resistance appeared exclusively in Gram-negative bacteria such as *E. cloacae* and *S. typhimurium*, and is due to either genetic mutations or horizontal gene transfer.[7] In the first case, the phenotypic outcomes correspond to both outer membrane porin (OmpC and OmpF) deficiency and CusCFBA transporter expression. The latter, firstly described as copper efflux machinery, has also been shown to carry out silver externalization. This transporter shows more than 80% identities with its pMG101 encoded homologue, the SilCFBA transporter.[8] Although these two Ag+ efflux systems are closely related and contain a similar set of proteins, the SilCFBA transporter is associated with another small protein, SilE, which has no counterpart in the copper efflux pump, and which seems to avoid the need for porin deficiency.[7,9] Even if the exact function of SilE is still unknown, these discoveries suggest an important role of this protein in Ag+ detoxification. Apart from SilE, the proteins involved in the Cus and Sil systems are known

Fig. 1 Amino acid sequence of SilE. The twenty first amino acids (blue) correspond to the signal peptide. The nine His- and Met-containing motifs (red) are studied as model peptides for the MX_2H and HX_nM motifs. The A79-G92 segment (underlined in green) corresponds to the sequence of the model peptide LP1.

to have defined functions.[10–13] The primary structure of SilE consists of 143 amino acids, including an N-terminal signal peptide of 20 amino acids that is cleaved after the periplasm targeting (Fig. 1). A first model of SilE has been proposed by Silver *et al.* where the protein binds silver ions exclusively *via* the histidine residues.[9] These first suggestions on the coordination properties of SilE were based on 1D ¹H NMR studies, showing shifts of histidine imidazole proton resonances upon Ag+ binding. However, this interpretation might be inadequate since the Ag+-mediated α-helix folding of SilE also alters the chemical shifts substantially.[14] A more detailed model of SilE has been put forward by Asiani *et al.* in which the protein is proposed to bind up to eight silver ions, using its 21 histidine and methionine residues.[14] Indeed, methionine is involved in Cu+ and Ag+ binding in a number of proteins, as the copper resistance protein CusF or the copper transporter Ctr1.[15,16] The histidine and methionine participation in Ag+ coordination in SilE was shown by investigating the amount of Ag+ coordinated by SilE mutants, in comparison with the wild type.[14] The sequence of SilE shows that these amino acids form nine MX_2H and HX_nM (n = 1, 2) motifs (Fig. 1). Together, these short sequences form two longer motifs, $MX_2HX_6HX_2M$ and $HX_2MX_3HX_2M$, repeated twice in the protein sequence. Two of these motifs (H80-M90 and M108-M121) have been identified to be crucial for the Ag+-mediated α-helix folding of the protein.[14] Although these previous studies proposed an implication of the histidine and methionine containing motifs in silver coordination, a severe lack of knowledge remains in

a Univ. Fribourg, Department of Chemistry, Chemin du Musée 9, 1700 Fribourg, Switzerland. E-mail: katharina.fromm@unifr.ch

b Univ. Lyon, CNRS, UCB Lyon 1, ENS-Lyon, Institut des Sciences Analytiques, UMR 5280, 5 rue de la Doua, 69100 Villeurbanne, France

c Univ. Grenoble Alpes, CNRS, CEA, LCBM (UMR 5249), F-38000 Grenoble, France

d Univ. Fribourg, Fribourg Center for Nanomaterials, FriMat, Chemin du Musée 9, 1700 Fribourg, Switzerland

terms of coordination numbers and geometries, binding affinities and tertiary structure of holo-SilE. Based on model peptide studies, we evidence here the role of histidine and methionine residues of SilE in silver coordination, and we provide silver binding affinities of the different binding sites of SilE, allowing us to offer a novel physiological role for the protein.

The nine MX_2H and HX_nM motifs have been synthesized as N-terminal acetylated, C-terminal amidated peptides (Ac-MX_2H-NH_2 and Ac-HX_nM-NH_2). Thereafter, the peptides are named by their single-letter amino acid code only (HQM, MDQH, MNEH, HETM, HEFM, HQKM, HQRM, HQAM and HRRM). ^{1}H and ^{13}C NMR studies of Ag^+ coordination using the herein described models have been performed in order to characterize the complexes in terms of stoichiometry, silver environment and affinity constant.

Indeed, the silver coordination by the peptides results in a more or less strong shifting of the His-$H^{\delta2}$ and His-$H^{\epsilon1}$ imidazole resonances (0.004 ppm $< |\Delta\delta(\text{His-H}^{\delta2})| < 0.182$ ppm; 0.008 ppm $< |\Delta\delta(\text{His-H}^{\epsilon1})| < 0.216$ ppm), either by shielding or deshielding of the signals, depending on the signal (His-$H^{\delta2}$ or His-$H^{\epsilon1}$) (Fig. 2a), and on the model (Fig. S1–S8, ESI†). These differences are likely to be the result of different peptide foldings, as they could not be assigned to different imidazole tautomeric forms, since only one tautomer has been identified from the ^{1}H, ^{13}C-HSQC spectra (Fig. S9a, ESI†), where all of the nine peptide complexes showed His-$C^{\delta2}$ resonances of around 117 ± 0.2 ppm, indicating a predominance of the His-$N^{\epsilon2}$–H tautomer.[17] The histidine involvement in the Ag^+ coordination sphere has been additionally confirmed by the deshielding of the His-C^{β} resonance during the complexation process (Fig. S2b, ESI†). The different shifts ($\Delta\delta$) evidence a fast chemical exchange in comparison with the NMR time scale, allowing the titration of the peptides by Ag^+.[18] Using this procedure, all models have been shown to form $1:1$ Ag^+/peptide complexes. As an example, the addition of Ag^+ to a solution of HETM results in a shift of $\delta2$ and $\epsilon1$ imidazole protons until 1 eq. of Ag^+ ($|\Delta\delta(\text{His-H}^{\delta2})| = 0.107$ ppm; $|\Delta\delta(\text{His-H}^{\epsilon1})| = 0.118$ ppm) (Fig. 2a). The stoichiometry of each complex has been confirmed by ESI-MS (Table S3, ESI†). The ^{1}H NMR titration of the different models has also allowed the observation of the chemical shift variations of the methionine methyl proton resonances ($|\Delta\delta(\text{Met-H}^{\epsilon})| = 0.420$ ppm ± 0.027) upon Ag^+ addition (Fig. 3a and Table 1). A similar experiment performed with a saturated solution of L-methionine alone leads to a similar downfield shift of the methyl proton resonance ($|\Delta\delta(\text{Met-H}^{\epsilon})| = 0.325$ ppm). Moreover, single crystals of the silver–methionine complex were obtained from this solution after one day, and the crystal structure has been solved by single crystal X-ray analysis (Fig. 4). The silver–methionine solid state structure displays a trigonal silver coordination sphere with one carboxylate and two thioether ligands. This attests
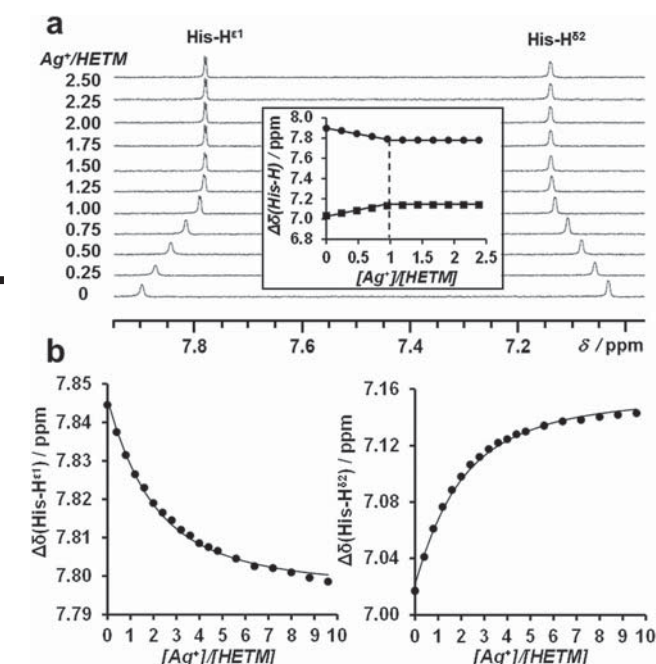

Fig. 2 HETM histidine ^{1}H NMR titrations. (a) Histidine imidazole ^{1}H resonance shift by the addition of $AgClO_4$ (0 to 1.25 mM) to a solution of HETM (500 μM) in HEPES buffer (20 mM, pD 7.8). The inset depicts the $1:1$ silver/peptide stoichiometry of the AgHETM complex formed based on His-$H^{\epsilon1}$ (circle) and His-$H^{\delta2}$ (square) resonance shift. (b) Plots of the histidine imidazole ^{1}H resonance shift by the addition of $AgClO_4$ (0 to 4.36 mM) to a solution of HETM (500 μM) in competition with imidazole-d4 (17.35 mM, pD 7.8). The solid lines correspond to the fits obtained using DynaFit, which yielded $\log K_{\text{ass}} = 6.4 \pm 0.1$.[24]

Fig. 3 HETM methionine ^{1}H NMR titrations. (a) Methionine methyl ^{1}H resonance (Met-H^{ϵ}) shift by the addition of $AgClO_4$ (0 to 1.25 mM) to a solution of HETM (500 μM) in HEPES buffer (20 mM, pD 7.8). (b) Plots of the methionine H^{ϵ} [1]H resonance shift by the addition of $AgClO_4$ (0 to 4.36 mM) to a solution of HETM (500 μM) in competition with imidazole-d4 (17.35 mM, pD 7.8). The solid line corresponds to the fit obtained using DynaFit, which yielded $\log K_{\text{ass}} = 6.4 \pm 0.1$.[24] (c) ^{1}H, ^{13}C-HSQC NMR spectra of HETM (red) and AgHETM (blue).
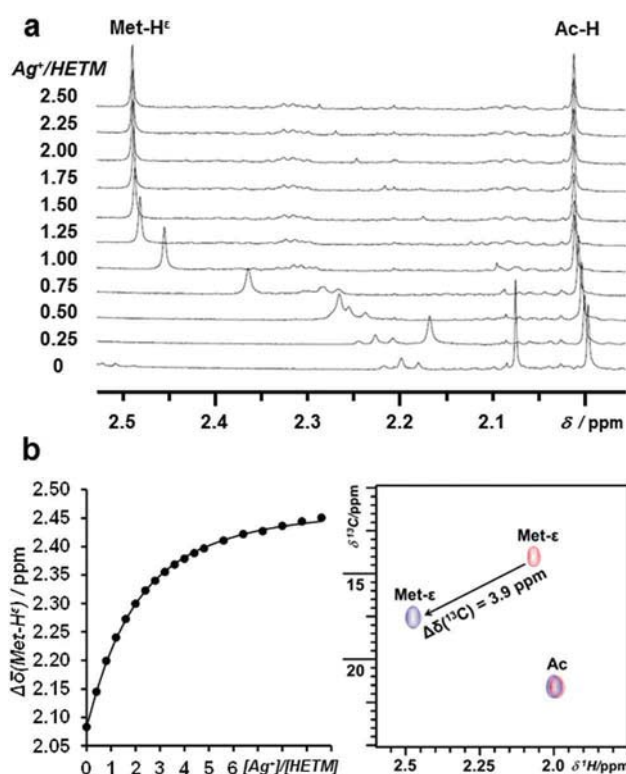
Table 1 ^{1}H NMR shifts and binding constants of the 1:1 Ag$^+$/peptide complexes

Model	$|\Delta\delta(\text{His-H}^{\varepsilon 1})|^a$	$|\Delta\delta(\text{His-H}^{\delta 2})|^a$	$|\Delta\delta(\text{Met-H}^{\varepsilon})|^a$	$\log K_{ass}{}^b$
His	0.101	0.109	—	—
Met	—	—	0.325	—
HQM	0.055	—	0.432	5.6
MDQH	0.216	0.004	0.415	5.8
MNEH	0.214	0.015	0.424	5.4
HETM	0.118	0.107	0.413	6.4
HEFM	0.099	0.140	0.447	6.6
HQKM	0.017	0.156	0.414	5.7
HQRM	0.041	0.167	0.417	5.5
HQAM	0.008	0.147	0.414	5.9
HRRM	0.081	0.165	0.406	5.3

^{a} The ^{1}H NMR shifts ($\Delta\delta$) correspond to maximal values of the peptide titration by AgClO$_4$. ^{b} $\log K_{ass}$ values ($\pm$ 0.1) are extracted from competition experiments using imidazole-d$_4$ (using Ag(imidazole)$_n$ (n = 1, 2) binding constants from Czoik et al.).[19]

that the deshielding of the Met-H$^{\varepsilon}$ resonance observed in the ^{1}H NMR spectrum is the result of Ag$^+$ coordination by the methionine S$^{\delta}$ atom. In addition to the deshielding of the Met-H$^{\varepsilon}$ signal, the complexation of Ag$^+$ by HETM results in a downfield shift of the Met-C$^{\varepsilon}$ resonance in the ^{1}H, ^{13}C-HSQC spectrum (Fig. 3c), which can be unequivocally assigned to the complexation of Ag$^+$ by the methionine. Indeed, Bersch et al. have reported a $\Delta\delta(\text{Met-C}^{\varepsilon})$ value of 2–5.5 ppm in SilB when the methionine residues were bound to Ag$^+$.[20] In the herein described systems, the Ag$^+$ binding to the methionine of each ultrashort peptide induces a similar downfield shift of the Met-C$^{\varepsilon}$ resonance of 3.9 ppm. By comparison, the N-terminal acetyl methyl carbon resonance (Ac-C) and the Thr-C$^{\gamma}$ are not affected by the silver complexation (Fig. 3c and Fig. S9b, ESI†). An additional proof of methionine coordination was obtained by reacting the free and Ag$^+$-bound peptides with an excess of H$_2$O$_2$. While the free peptide was converted into a sulfoxide, the Ag$^+$-bound peptide was not oxidized, suggesting that the methionine sulfur of the latter was not available for reaction with H$_2$O$_2$ (Fig. S10, Tables S2 and S3, ESI†). The ^{1}H NMR titration curves of the different peptides by Ag$^+$ show sharp end

points indicative of a tight binding. Since the saturation at 1 eq. of Ag$^+$ exceeds 80%, the binding constants cannot be extracted from these direct titrations.[21,22] Accurate binding constants have thus been determined from Ag$^+$ titrations of the peptides in competition with imidazole-d4 (5.2 $< \log K_{ass}(\text{AgHX}_n\text{M}) <$ 6.6; 5.4 $< \log K_{ass}(\text{AgMX}_2\text{H}) <$ 5.8) (Table 1).[19,23,24] The binding constants were extracted from Met-H$^{\varepsilon}$ ^{1}H NMR resonance shifts for all complexes and from His-H$^{\delta 2}$ and/or His-H$^{\varepsilon 1}$ ^{1}H resonance shifts when $\Delta\delta \geq$ 0.05 ppm (Table S1, ESI†). For each complex, the $\log K_{ass}$ values obtained from the different ^{1}H resonances differ by not more than 4%. This attests to the coordination of one Ag$^+$ by both amino acids in each model. The higher affinities observed for AgHETM and AgHEFM ($\log K_{ass}(\text{AgHETM})$ = 6.4; $\log K_{ass}(\text{AgHEFM})$ = 6.6) suggest a potential glutamate participation in the silver coordination sphere, in particular if in proximity of histidine. Indeed, the Glu-C$^{\beta}$ and Glu-C$^{\gamma}$ resonances are upfield shifted upon Ag$^+$ complexation (Fig. S9b, ESI†). This is also consistent with the silver–methionine crystal structure which features a mixed thioether-carboxylate Ag$^+$ binding site (Fig. 4).

In order to confirm the Ag$^+$ binding mode on a longer segment of SilE, a model peptide (LP1) containing two HX$_2$M motifs has been studied (Fig. 1). Based on NMR and CD studies, we could show that LP1 can bind two silver ions via its two HX$_2$M motifs, inducing a folding of the peptide in the α-helix (Fig. 5). Indeed, each His-H$^{\varepsilon 1}$ and His-H$^{\delta 2}$ resonance and two of the three Met-H$^{\varepsilon}$ resonances are deshielded upon Ag$^+$ addition before a plateau is reached after the addition of 2 eq. of Ag$^+$ (Fig. 5 and Fig. S13, ESI†). Although the third Met-H$^{\varepsilon}$ resonance is also deshielded during the titration, this shift is continuous and seems to be the result of a weak interaction. This is therefore consistent with a binding of one Ag$^+$ by each HX$_2$M motif.

Within the framework of understanding of the bacterial resistance against Ag$^+$, these results bring new insights into the interaction of SilE with Ag$^+$. Indeed, the former is the last component of the Sil system whose exact role is still unknown, although it has been stated to be mandatory to provide resistance.[7] The use of short model peptide "cut out" from the parent protein constitutes thus a powerful method to learn
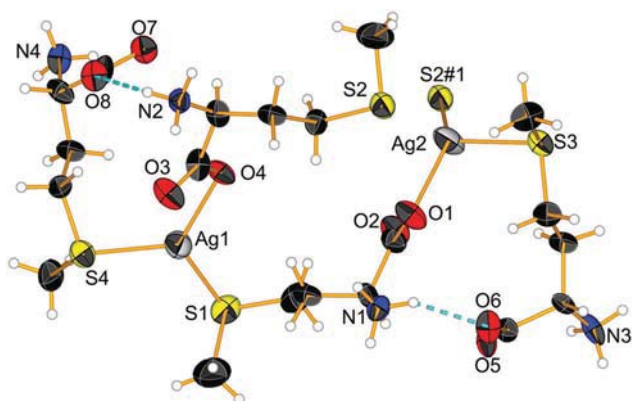

Fig. 4 Crystal structure of {[Ag$_2$(L-methionine)$_4$](NO$_3$)$_2$·2H$_2$O}$_n$. Nitrate anions and water molecules were omitted for clarity. Ellipsoids are drawn at 50% of probability. Hydrogen bonds are represented as blue dashed lines. Symmetry operator: #1 x + 1, y, z.
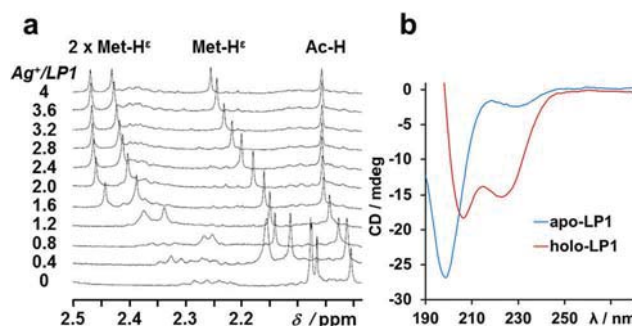

Fig. 5 LP1 ^{1}H NMR titration and CD spectra. (a) Methionine methyl ^{1}H resonance (Met-H$^{\varepsilon}$) shift by the addition of AgClO$_4$ (0 to 2 mM) to a solution of LP1 (500 µM) in deuterated HEPES buffer (20 mM, pD 7.8). (b) Circular dichroism spectra of apo-LP1 (blue) and holo-LP1 (red). Addition of AgClO$_4$ (120 µM) to a solution of LP1 (30 µM, pH 7.4) induces a folding of LP1 into an α-helix.
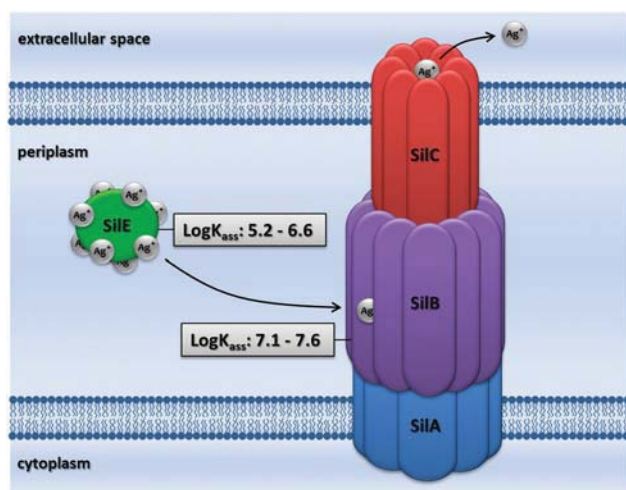
Fig. 6 Schematic representation of the potential silver ion transfer between the periplasmic protein SilE and the periplasmic adaptor protein SilB, based on the silver affinity gradient between SilE and SilB. $\log K_{ass}$ values correspond to the values obtained from competition experiments of the current study for SilE and to the lower limit values determined by Urbina *et al.* for SilB.[26]

about protein–metal interactions, reminiscent of previous studies on protein–protein interactions.[25] Indeed, the study of the herein described models of SilE not only proved the histidine and methionine involvement in Ag^+ coordination, but also allowed the determination of the Ag^+ affinity for several sites of the protein. With $\log K_{ass}$ values comprised between 5.2 and 6.6, these short motifs display moderately strong affinities for silver ions. Nevertheless, these affinities could be slightly higher in the whole protein, by means of cooperative binding, and second-sphere coordination effects. As a comparison, a cyclic peptide modelling of the CusF chaperone protein binding site shows a $\log K_{ass}$ of 7.3 for a silver binding site composed of two methionine, one histidine, and one tryptophan moieties, the latter providing a cation–π interaction.[23] The periplasmic adaptor of the SilCBA transporter, SilB, features a silver binding site composed of three methionine residues in its N-terminal domain, and a CusF-like silver binding site in its C-terminal domain. Both domains also display high affinity for Ag^+ with lower limits of $\log K_{ass}$ values of 7.1 and 7.6 for the N-terminal and C-terminal sites respectively, as determined by ITC.[26] With only one methionine and one histidine residue, the nine MX_2H and HX_nM silver binding sites of SilE possess hence weaker affinities and could therefore transfer free silver ions to each domain of SilB, by means of silver affinity gradient between the two partners (Fig. 6). When saturated, the latter could in turn transfer silver ions to the SilA efflux pump for externalization.[26] Furthermore, two "core-motifs" have been previously identified to be the first nucleation sites of SilE for the Ag^+-mediated folding.[14] The HEFM motif, which shows the highest affinity for silver ions ($\log K_{ass}$ = 6.6), is a part of one of these segments (M108-M121). On the other hand, investigation of the Ag^+ coordination by the nine MX_2H and HX_nM motifs separately allows suppositions about the Ag^+/SilE stoichiometry. Indeed, while Silver *et al.* reported a binding of 5–38 Ag^+ by SilE, Asiani *et al.* suggested that SilE could only bind

a maximum of 8 Ag^+.[14,27] The 1:1 Ag^+/peptide stoichiometry of the nine herein described models is closer to this second assumption, as it suggests a maximum of 9 Ag^+ bound to the protein.

In conclusion, using short model peptides, we proved the presence of nine possible silver binding sites in SilE, in which silver ions are coordinated by the histidine and methionine side chains. Furthermore, their range of affinity ($10^{5.2}$–$10^{6.6}$), which is lower than that of SilB binding sites, suggests an Ag^+ buffering role of SilE, before the transfer to SilB for export, rather than an Ag^+ sequestration role. Since it appeared that further side groups, *e.g.* glutamic acid, might as well contribute to the coordination of silver ions, the structure elucidation and the binding constant determination of longer model peptides for SilE are currently ongoing in our group. The latter will allow us to find out whether SilE binds several silver ions in a cooperative or sequential binding mode. This work is thus a first important step to the structure elucidation of SilE and provides new insights into its physiological role.

Notes and references

1 H. J. Klasen, *Burns*, 2000, **26**, 117.
2 H. J. Klasen, *Burns*, 2000, **26**, 131.
3 E. M. Hetrick and M. H. Schoenfisch, *Chem. Soc. Rev.*, 2006, **35**, 780.
4 A. T. Hendry and I. O. Stewart, *Can. J. Microbiol.*, 1979, **25**, 915.
5 C. Jelenko, *Ann. Surg.*, 1969, **170**, 296.
6 S. L. Percival, P. G. Bowler and D. Russell, *J. Hosp. Infect.*, 2005, **60**, 1.
7 C. P. Randall, A. Gupta, N. Jackson, D. Busse and A. J. O'Neill, *J. Antimicrob. Chemother.*, 2015, **70**, 1037.
8 M. Zimmermann, S. R. Udagedara, C. Ming Sze, T. M. Ryan, G. J. Howlett, Z. Xiao and A. G. Wedd, *J. Inorg. Biochem.*, 2012, **115**, 186.
9 S. Silver, *FEMS Microbiol. Rev.*, 2003, **27**, 341.
10 F. Long, C.-C. Su, M. T. Zimmermann, S. E. Boyken, K. R. Rajashankar, R. L. Jernigan and E. W. Yu, *Nature*, 2010, **467**, 484.
11 C.-C. Su, F. Yang, F. Long, D. Reyon, M. D. Routh, D. W. Kuo, A. K. Mokhtari, J. D. Van Ornam, K. L. Rabe, J. A. Hoy, Y. J. Lee, K. R. Rajashankar and E. W. Yu, *J. Mol. Biol.*, 2009, **393**, 342.
12 Y. Xue, A. V. Davis, G. Balakrishnan, J. P. Stasser, B. M. Staehlin, P. Focia, T. G. Spiro, J. E. Penner-Hahn and T. V. O'Halloran, *Nat. Chem. Biol.*, 2008, **4**, 107.
13 R. Kulathila, R. Kulathila, M. Indic and B. van den Berg, *PLoS One*, 2011, **6**, e15610.
14 K. R. Asiani, H. Williams, L. Bird, M. Jenner, M. S. Searle, J. L. Hobman, D. J. Scott and P. Soultanas, *Mol. Microbiol.*, 2016, **101**, 731.
15 J. T. Rubino, P. Riggs-Gelasco and K. J. Franz, *JBIC, J. Biol. Inorg. Chem.*, 2010, **15**, 1033.
16 A. V. Davis and T. V. O'Halloran, *Nat. Chem. Biol.*, 2008, **4**, 148.
17 J. L. Sudmeier, E. M. Bradshaw, K. E. Coffman Haddad, R. M. Day, C. J. Thalhauser, P. A. Bullock and W. W. Bachovchin, *J. Am. Chem. Soc.*, 2003, **125**, 8430.
18 C. D. Syme and J. H. Viles, *Biochim. Biophys. Acta*, 2006, **1764**, 246.
19 R. Czoik, A. Heintz, E. John and W. Marczak, *Acta Phys. Pol., A*, 2008, **114**, 51.
20 B. Bersch, K.-M. Derfouri, F. De Angelis, V. Auquier, E. N. Ekendé, M. Mergeay, J.-M. Ruysschaert and G. Vandenbussche, *Biochemistry*, 2011, **50**, 2194.
21 P. Thordarson, *Chem. Soc. Rev.*, 2011, **40**, 1305.
22 D. A. Deranleau, *J. Am. Chem. Soc.*, 1969, **91**, 4044.
23 M. Isaac, S. A. Denisov, A. Roux, D. Imbert, G. Jonusauskas, N. D. McClenaghan and O. Sénèque, *Angew. Chem., Int. Ed.*, 2015, **54**, 11453.
24 P. Kuzmič, *Anal. Biochem.*, 1996, **237**, 260.
25 H. Benyamini and A. Friedler, *Future Med. Chem.*, 2010, **2**, 989.
26 P. Urbina, B. Bersch, F. De Angelis, K.-M. Derfoufi, M. Prévost, E. Goormaghtigh and G. Vandenbussche, *Biochemistry*, 2016, **55**, 2883.
27 A. Gupta, K. Matsui, J. F. Lo and S. Silver, *Nat. Med.*, 1999, **5**, 183.